Critical Phenomena under Shear Flow

Pavlik Lettinga, Hao Wang, Jan K.G. Dhont

Close to a gas-liquid critical point, effective interactions between particles become very long ranged, and the dynamics of concentration fluctuations is very slow (commonly referred to as "critical slowing down"). The long ranged interactions lead to the so-called critical structure factor, which can be observed with light scattering. The long ranged interactions and the critical slowing down renders the microstructure of a near critical system very sensitive to shear flow: microstructural response is non-linear for relatively small shear rates and an out-of-phase component of the response to oscillatory shear flow is present already at small frequencies. Non-linear viscoelastic response therefore occurs at small shear rates and frequencies.

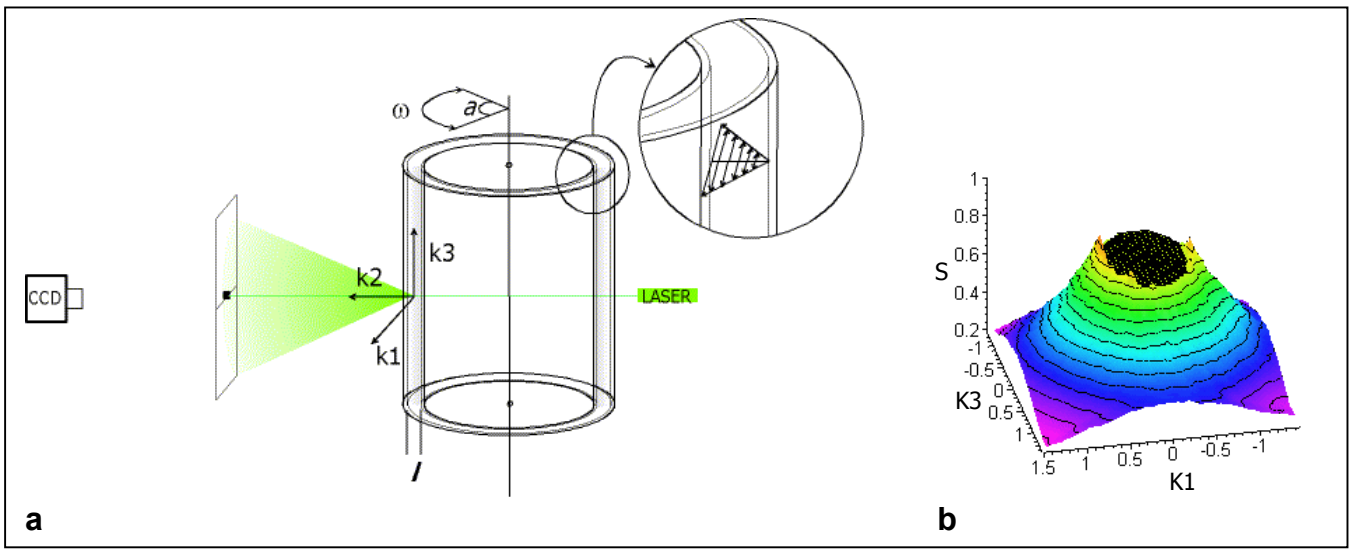

Fig. 1a) Schematic drawing of the experimental set-up for Small-Angle Light Scattering experiments under shear. K1 is the flow direction,K2 is the gradient direction, and K3 the vorticity direction. b) Critical structure factor of a colloid-polymer mixture as measured Small Angle Light Scattering. The Z-axis denotes the scatter intensity.

Examples of critical colloidal systems : Two kinds of colloidal systems have been used so far to investigate critical phenomena under shear flow : silica spheres coated with stearyl alcohol, dissolved in benzene and silica spheres mixed with polymer (polydimethylsiloxane) in cyclohexane. Since benzene is a marginal solvent for stearyl alcohol, these alcohol chains on two different colloidal spheres rather overlap with each other than separately dissolve in benzene. This leads to a short range attractive pair-interaction potential, the depth of which is temperature dependent due to the variation in quality of the solvent (benzene) for stearyl alcohol. The temperature-concentration phase diagram of this system is shown in the left figure below. There is a bimodal, spinodal and a gel-line which intersects with the gas-liquid critical point. Besides studying critical phenomena, this system allows to investigate microstructural order around the gel-line and the effects of shear flow, and the influence of gellation forces on critical phenomena. In fact we observed an increase in the turbidity on applying shear flow in the vicinity of the gel-line and a decrease near the critical point somewhat away from the gel-line. A relatively easy way to establish a critical point is to add polymers to a system of hard colloidal spheres. Part of the phase diagram of such a system is

given in the right figure below. Instead of the temperature, the control variable is now the concentration of polymer. The critical point can be approached along a so-called dilution line (indicated in the figure) by simple evaporating solvent. See for further reading Verduin and Dhont.[1]

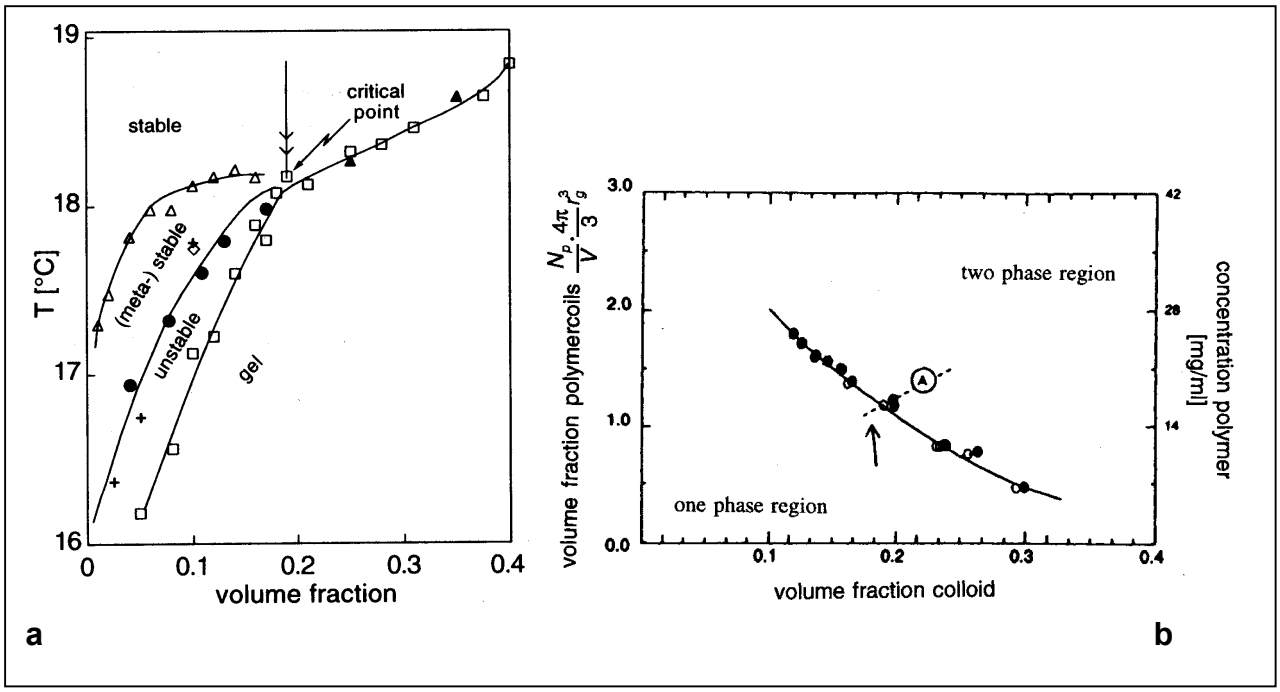

Fig. 2: a) Phase diagram stearyl grafted silica spheres in benzene system.
b) Phase diagram colloid/polymer mixture

Critical divergence of viscoelastic response functions : The development of very long ranged correlation on approach of the gas-liquid critical point gives rise to the divergence of, for example, viscoelastic response functions. These response functions are directly related to the structure factor response described above. For a colloid polymer mixture under stationary shear flow the shear viscosity is found to diverge with the same exponent as the correlation length (see the figure below). This very much stronger divergence for colloidal systems as compared to atomic/molecular systems is due to the very long ranged hydrodynamic interactions between the colloidal particles. See for further reading Bodnár[3] and Dhont.[2]

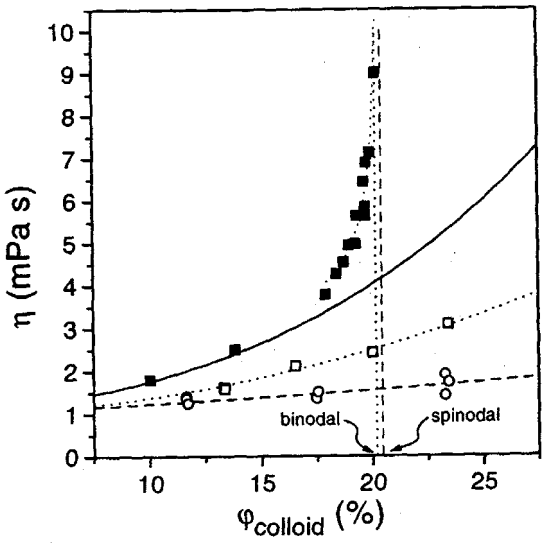

Fig. 3: Divergence of the viscosity

Critical microstructure under static shear flow : The microstructure of a system is quantified by the static structure factor S(**k**), which is essentially the Fourier transform of the pair-correlation function. For systems under shear flow the structure factor is anisotropic, that is, the structure factor is a function of the direction of the wavevector **k**, not just of it's magnitude as for isotropic systems. The anisotropic nature of the structure factor leads to dichroism, which can be used to test theories for structure factors under shear flow,[3] as well as direct observation of the scattered light. The structure factor can be calculated from the N-particle Smoluchowski equation, with the neglect of hydrodynamic interaction and to within the approximation involved in the closure relation for the 3-particle correlation function (a modified superposition approximation). Within the mean-field region (where equations of motion for the pair-correlation function g can be linearized with respect to the long-ranged part of the pair-correlation function around g=1) one finds that under stationary shear flow the structure factor is equal to,

$$S^{\mathrm{stat}}(\mathbf{K}) = S^{\mathrm{eq}}(K)\left[1+\frac{1}{\lambda K_1}\int_{K_2}^{\pm\infty} dX\left[K^2-K_2^2+X^2\right]\times\left[K_2^2-X^2\right]\exp\left\{-\frac{F(\mathbf{K}\mid X)}{\lambda K_1}\right\}\right],$$

with the upper integration limit equal to $+\infty$ for $\lambda K_1>0$, and $-\infty$ for $\lambda K_1<0$.
The equilibrium structure factor $S^{\mathrm{eq}}(K)$ is given by

$$S^{\mathrm{eq}}(k) = \frac{1}{\beta\Sigma}\frac{\xi^2}{1+(k\xi^2)}, \text{ and } F \text{ equals } F(\mathbf{K}\mid X) = \int_{K2}^{X} dY\,[K^2-K_2^2+Y^2][1+K^2-K_2^2+Y^2].$$

ξ is defined as the correlation length, given by

$$\xi = \sqrt{\Sigma \Big/ \frac{d\Pi}{d\rho}},$$

where Σ is the Cahn-Hilliard square gradient coefficient, Π the osmotic pressure, and $\bar{\rho}$ the average particle density. The dimensionless wave vector **K** is given by **K** = ξ·**k**, and λ is the "dressed Péclet number" defined as

$$\lambda = \dot{\gamma}\,\frac{\xi^2}{2D^{eff}(k=0)},$$

where D^{eff} if the effective diffusion coefficient at k=0 given by $D^{eff}(\mathrm{k}=0)=D_0\beta\Sigma$.

The effect of shear on the structure factor is demonstrated in Fig. 4, where we sheared a system similar to that described above (*Critical divergence of viscoelastic response functions*). Here the change in the structure factor along the flow direction and along the vorticity direction is shown for different shear rates and wave-vectors. The data could be fitted nicely with the parameter λ and two additional parameters α and ε, which account for the shear rate dependent distortion of the short-ranged part of the pair correlation function. The results for the fit at different correlation lengths are given in Fig. 9. See for further reading Wang et al.[4]

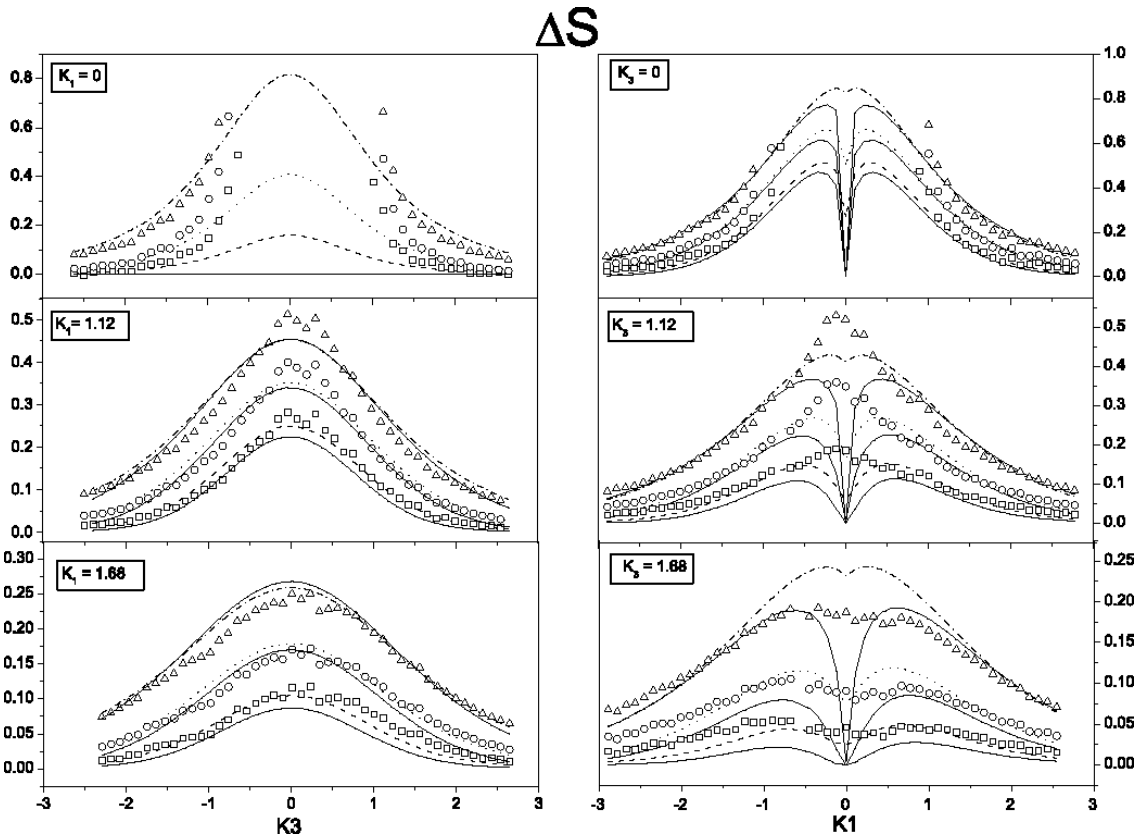

Fig. 4: Typical fitting results for a correlation length 1500 nm for three shear-rates: $\dot{\gamma} = 20.46\ s^{-1}$ *(Δ and dash-dot line);* $\dot{\gamma} = 8.7\ s^{-1}$ *(○ and dotted line);* $\dot{\gamma} = 1.84\ s^{-1}$ *(□ and dashed line). The values for the wavevectors indicated in the figures are the wavevectors where cross-sections are taken, as indicated by the thick lines in Fig. 1. The solid lines are the best fit to the older theory, where distortion of short-ranged correlations is neglected . Note the difference in scale of the vertical axis for the different cross-sections.*

Critical microstructure under oscillatory shear flow : Our current research is focused on the non-linear viscoelastic behavior of colloidal dispersions. The non-linear response of an colloidal dispersion on a external applied filed is best studied using an oscillating shear flow. The time dependent static structure factor under oscillatory shear flow, after transients have died away, is equal to[5]

$$S^{\,\mathrm{osc}}(\mathbf{K},\tau) = S^{\mathrm{eq}}(K) - 2\frac{\lambda K_1}{\Omega}\int_{-\infty}^{\tau} d\tau' \cos\{\Omega\tau\}\frac{S^{\mathrm{eq}}(G_0(\tau'))}{1+G_0^2(\tau')}$$
$$\times\left[K_2 + \lambda K_1(\sin\{\Omega\tau\} - \sin\{\Omega\tau'\})\right]\times\exp\{-H_0(\tau')\}$$

with $H_0(\tau') = \int_{\tau'}^{\tau} G_0^2(\tau'')\left[1+G_0^2(\tau'')\right]$ and $G_0(\tau') = (K_1, K_2 + \frac{\lambda K_1}{\Omega}\left[\sin\{\Omega\tau\} - \sin\{\Omega\tau'\}\right], K_3)$

The dimensionless frequency Ω (or a "dressed Deborah number") and time τ are given by

$$\Omega = \omega\frac{\xi^2}{2D^{eff}(k=0)} \text{ and } \tau = t\frac{2D^{eff}(k=0)}{\xi^2}.$$

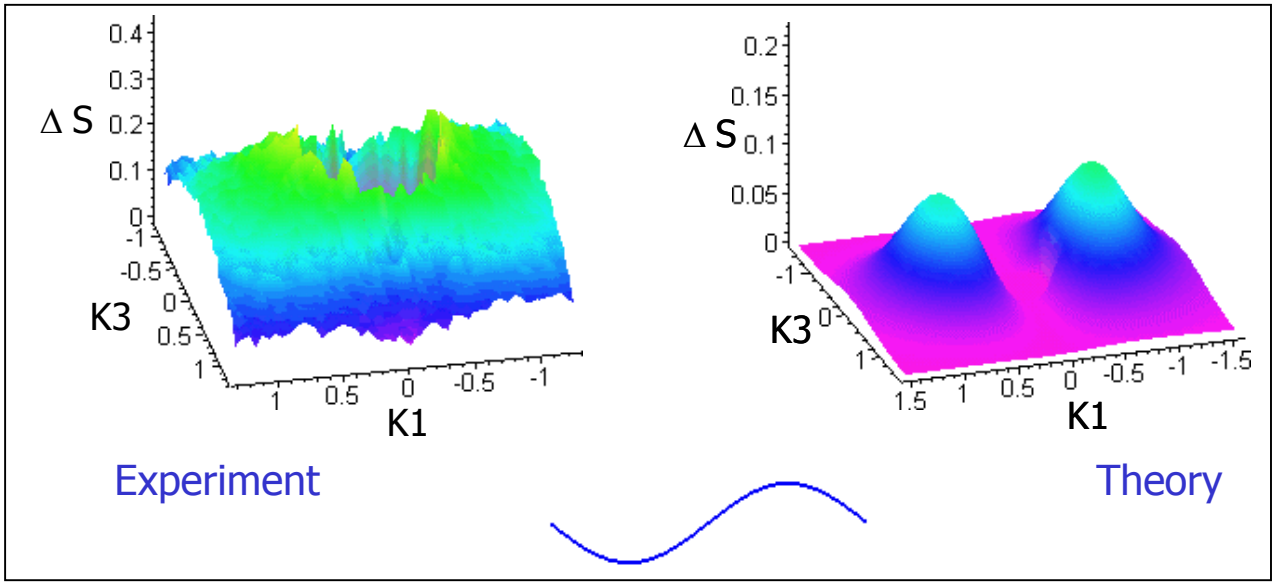

The effect of an oscillatory shear flow on the critical structure factor is demonstrated in the MOVIE, where the change in the structure factor is followed as a function of time. Some features can be readily deduced from this film, such as the increase in the phase shift for decreasing K-vectors, i.e. increasing structure size. Also it can be seen that the maximum distortion is found at a specific wave-vector. In order to gain more insight the, we performed a Fourier analysis per wave-vector as in Fig. 5. In this figure we varied the maximum shear rate. We see that at the highest shear rate higher harmonics appear, and hence that the response becomes more non-linear.

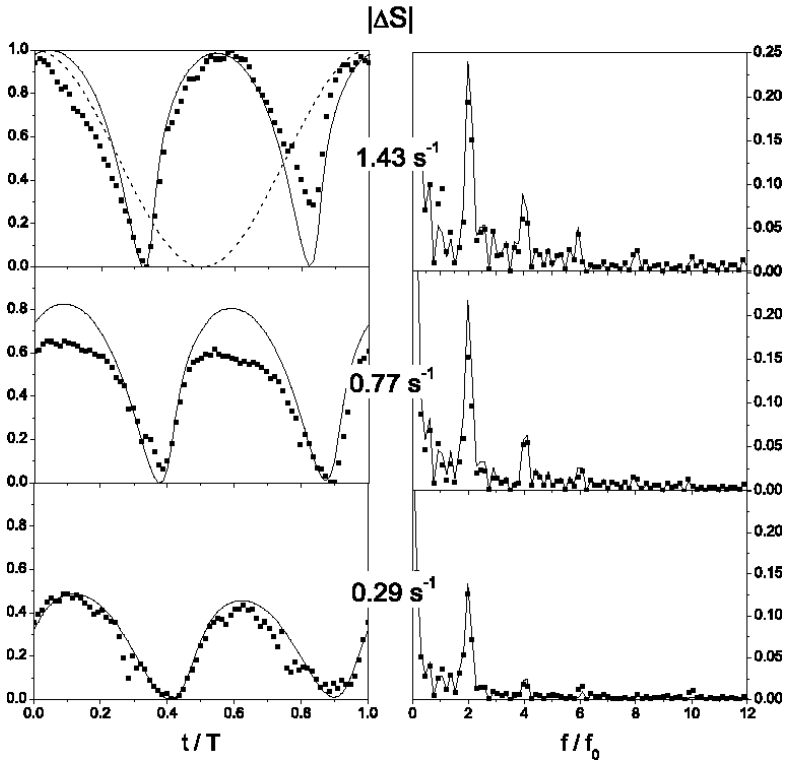

Fig. 5: The response a near-critical colloidal dispersion (ξ = 945nm) to an oscillatory shear flow in the time-domain (left) and frequency-domain (right), for $\omega = 2\pi 0.025\ s^{-1}$. The wave-vector component is taken along the flow directions (K1 = 1.4, K3 = 0). The symbols represent the experimental data. The solid lines indicate the theoretical prediction, using $\lambda/\dot{\gamma} = 0.6$. Both experimental data and theory are normalized with respect to the response of the highest shear rate. The dashed line represents the applied field.

In Fig. 6 we summarize the real, imaginary, and total response of the second harmonic for experiments (on the left) and theory (on the right). The K-dependence of the phase shift is clearly demonstrated in Fig. 6d and i. Taking a cut at K3=0, we vary the correlation length (Fig. 7a) and frequency (Fig. 7b). We show in this figure that the phase shift increases with increasing correlation length, which demonstrates that the Brownian diffusion is too slow to counterbalance the shear distortion for the increasing size of critical structures. The same counts for increase of the phase shift for increasing frequency.

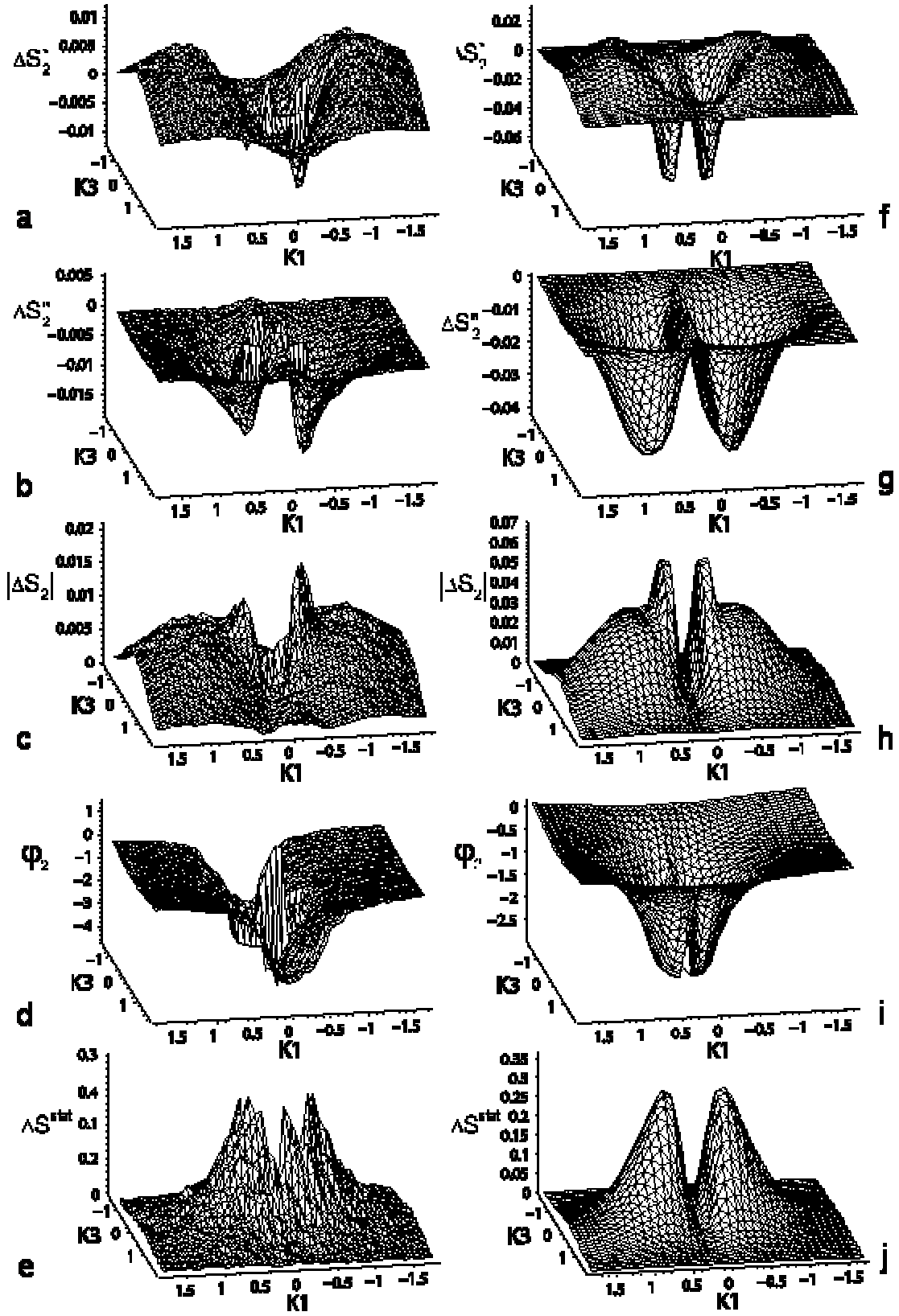

Fig. 6: All second harmonic responses of the structure factor for experiment (a to e) and theory (f to j), as found from the Fourier analysis. The experimental data were taken for $\dot{\gamma}_{max} = 0.68\ s^{-1}$ *and* $\omega = 2\pi 0.05\ s^{-1}$, *with* $\xi = 945$ *nm. The corresponding theoretical values are calculated using* $\lambda/\dot{\gamma} = 0.6$.

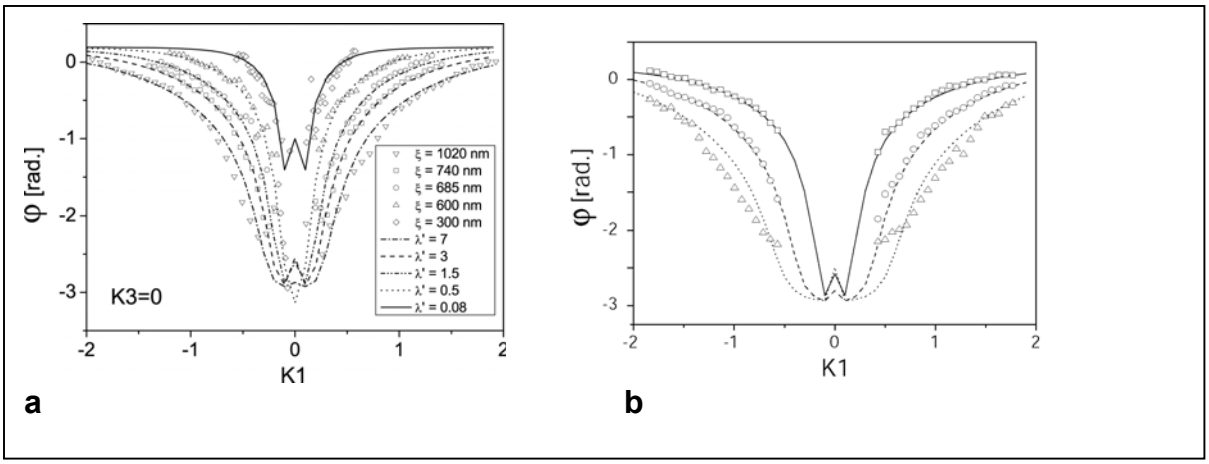

Fig. 7: a) The K1-dependence of the phase shift for varying correlation lengths at $\omega = 2\pi 0.5\ s^{-1}$ *and* $\dot{\gamma}_{max} = 1.0\ s^{-1}$ *. The symbols are the experimental data, the lines represent fits to the proportionality constant* $\lambda/\dot{\gamma}$ *, which is the only fit parameter. The results of the fit are plotted in Fig. 9. b) as a) but for varying frequency at a fixed shear rate (*$\dot{\gamma}_{max} = 0.8\ s^{-1}$ *): ω =* $2\pi\ 0.025 s^{-1}$ *(□),* $\omega = 2\pi 0.05 s^{-1}$ *(○),* $\omega = 2\pi 0.1 s^{-1}$ *(Δ). The lines indicate the theoretical prediction, using λ' = 0.6 to calculate Ω.*

The values of the fit-parameters for as well oscillatory shear and stationary shear experiments versus the critical correlation length ξ are plotted in Fig. 8. Independently of the results for stationary flow we also find for the oscillatory flow that the exponent in the ξ-dependence of $\lambda/\dot{\gamma}$ is of the order of 4. The slope we find is 3.7 ± 0.4.

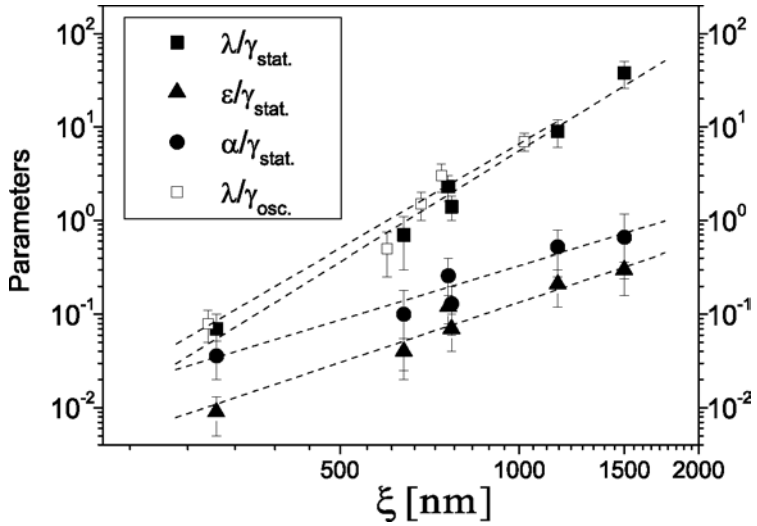

Fig. 9: The parameters $\lambda/\dot{\gamma}$ *,* $a/\dot{\gamma}$ *and* $\varepsilon/\dot{\gamma}$ *obtained from the fit of the stationary as well as oscillatory (only* $\lambda/\dot{\gamma}$ *) flow data, as a function of the correlation length.*

REFERENCES:

[1] H. Verduin and J. Dhont, *Phys. Rev. E* **52**, 1811 (1995).
[2] I. Bodnár and J. K. G. Dhont, *Phys. Rev. Lett.* **77**, 5304 (1996).
[3] T. A. J. Lenstra and J. K. G. Dhont, *Phys. Rev. E.* **63**, 61401 (2000).

[4] H. Wang, M. P. Lettinga, and J. K. G. Dhont, *J.Phys.:Condens.Matter* **14**, 7599 (2002).
[5] J. K. G. Dhont and G. Nägele, *Phys. Rev. E* **58**, 7710 (1998).